8022–8034 *Nucleic Acids Research, 2020, Vol. 48, No. 14* *Published online 23 June 2020*
doi: 10.1093/nar/gkaa522

METTL15 interacts with the assembly intermediate of murine mitochondrial small ribosomal subunit to form m^{4}C840 12S rRNA residue

Ivan Laptev[1,2,3,†], Ekaterina Shvetsova[4,†], Sergey Levitskii[5], Marina Serebryakova[1,3], Maria Rubtsova[1,2], Victor Zgoda[6], Alexey Bogdanov[2,3], Piotr Kamenski[5,*], Petr Sergiev[1,2,3,7,*] and Olga Dontsova[1,2,3,8]

[1]Center of Life Sciences, Skolkovo Institute of Science and Technology, Skolkovo, Moscow 143028, Russia, [2]Department of Chemistry, Lomonosov Moscow State University, Moscow 119992, Russia, [3]Belozersky Institute of Physico-Chemical Biology, Lomonosov Moscow State University, Moscow 119992, Russia, [4]Faculty of Bioengineering and Bioinformatics, Lomonosov Moscow State University, Moscow 119992, Russia, [5]Faculty of Biology, Lomonosov Moscow State University, Moscow 119992, Russia, [6]Institute of Biomedical Chemistry, Moscow 119435, Russia, [7]Institute of Functional Genomics, Lomonosov Moscow State University, Moscow 119992, Russia and [8]Shemyakin-Ovchinnikov Institute of Bioorganic Chemistry, Moscow 117997, Russia

Received July 09, 2019; Revised May 12, 2020; Editorial Decision June 06, 2020; Accepted June 08, 2020

ABSTRACT

Mammalian mitochondrial ribosomes contain a set of modified nucleotides, which is distinct from that of the cytosolic ribosomes. Nucleotide m^{4}C840 of the murine mitochondrial 12S rRNA is equivalent to the dimethylated m^{4}Cm1402 residue of *Escherichia coli* 16S rRNA. Here we demonstrate that mouse METTL15 protein is responsible for the formation of m^{4}C residue of the 12S rRNA. Inactivation of *Mettl15* gene in murine cell line perturbs the composition of mitochondrial protein biosynthesis machinery. Identification of METTL15 interaction partners revealed that the likely substrate for this RNA methyltransferase is an assembly intermediate of the mitochondrial small ribosomal subunit containing an assembly factor RBFA.

INTRODUCTION

Apart from the standard four nucleotides, RNA molecules are functionalized by a variety of nearly two hundred modified nucleotides (1). Such residues are present in the ribosomal RNA molecules of all species (2) and tend to be clustered in the functional centres of the ribosome (3,4). Apart from the cytosolic ribosomes, eukaryotes maintain additional independent ribosome species that are responsible for protein synthesis in mitochondria (5,6). Mutations in the genes coding for the components of human mitochondrial translation apparatus are among the causative factors of severe mitochondrial diseases (7), while inhibition of the mitochondrial ribosomes is one of the main causes of aminoglycoside antibiotics side effects (8,9). Mitochondrial ribosomes are structurally distinct from other types of ribosomes (10–12) and contain a set of modified nucleotides only marginally overlapping with that of the cytosolic ribosomes and resembling those of bacterial ones (2,13,14). Until recently complete list of enzymes responsible for the modification of mitochondrial ribosomal RNA was available only for yeast (13), an organism containing a relatively small number of methylated residues in the mitochondrial RNA (15).

Mammalian mitochondrial ribosomes contain the 12S rRNA residue m^{4}C840 (mouse numbering, human equivalent is m^{4}C839) (16) in a position, equivalent to the *Escherichia coli* 16S rRNA nucleotide m^{4}Cm1402 (Figure 1A). The modified m^{4}C840 nucleotide of the 12S rRNA (Figure 1A) is located in the decoding center of the mitochondrial small ribosomal subunit and is expected to interact with mRNA. Bacteria uses two distinct enzymes, RsmI and RsmH (17) for the methylation of the ribose 2′-hydroxyl and N4 amino group of the 16S rRNA residue C1402, respectively (Figure 1A). Curiously, eukaryotes retained ribose methylation at the 18S rRNA Cm1703 (human numbering) only for the cytosolic ribosomes, where this modification is introduced by a U43 snoRNA dependent mechanism (18). On the contrary, methylation of N4 amino group is specific for only mitochondrial, but not cytosolic ribosomes (Figure 1A).

*To whom correspondence should be addressed. Tel: +7 495 9395418; Fax: +7 495 9393181; Email: petya@genebee.msu.su
Correspondence may also be addressed to Piotr Kamenski. Tel: +7 495 9395485; Fax: +7 495 9393181; Email: peter@protein.bio.msu.ru
†The authors wish it to be known that, in their opinion, the first two authors should be regarded as Joint First Authors.

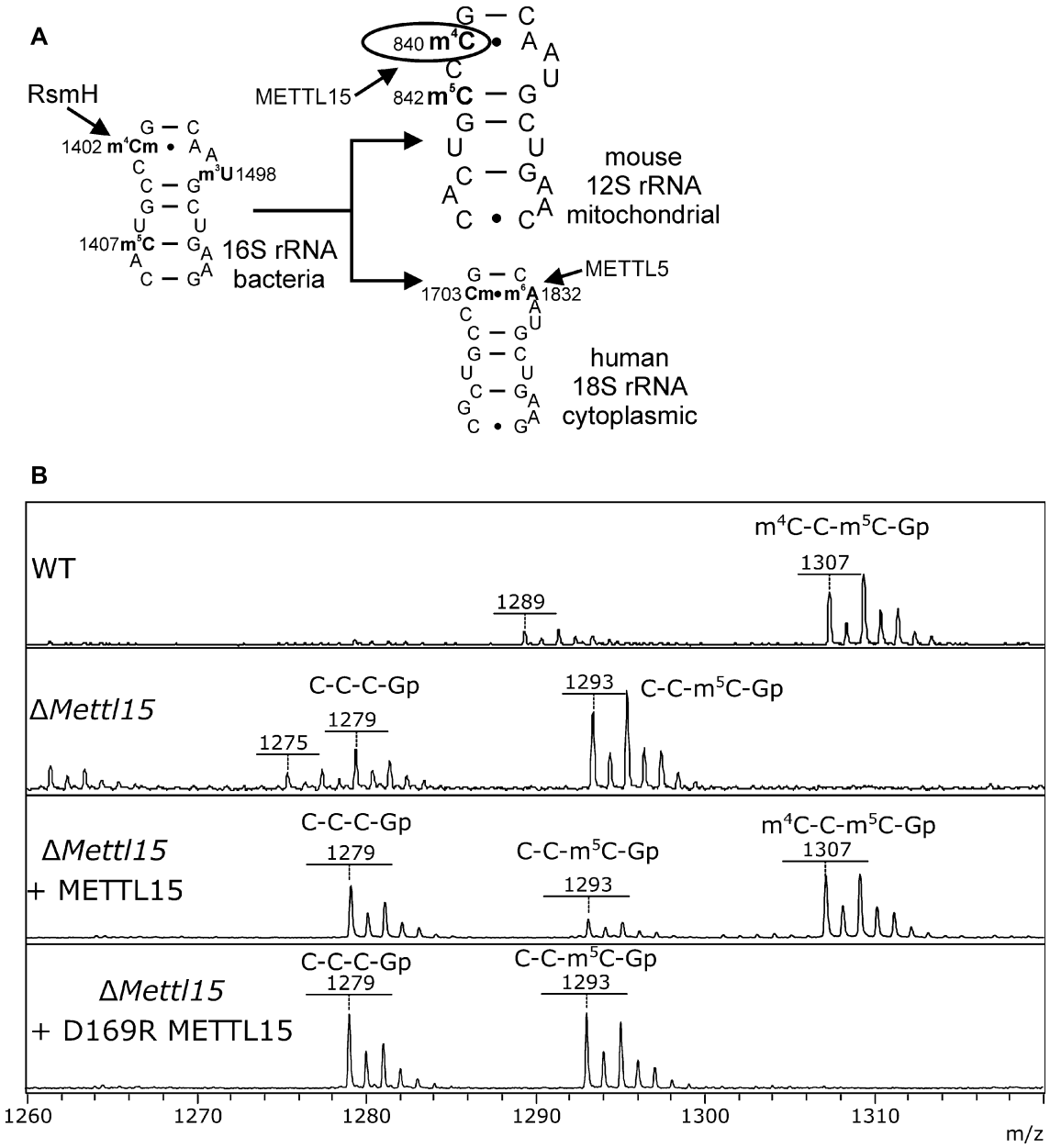

Figure 1. METTL15 methylate 12S rRNA. (**A**) Secondary structure of the upper part of helix 44 for the bacterial 16S rRNA (left panel), human cytosolic 18S rRNA (right lower panel) and mouse mitochondrial 12S rRNA (right upper panel). Modified nucleotides are shown in bold and labeled. Bacterial (RsmH) and eukaryal (METTL15) enzymes responsible for m^4C modification as well as METTL5 enzyme responsible for m^6A modification are shown. (**B**) Mass spectra of the 12S rRNA fragment with C840 nucleotide. Panels are labelled accordingly to the cell lines, i.e. 'WT' corresponds to the wild type NS0 cells, Δ*Mettl15* corresponds to the *Mettl15* knockout, while 'Δ*Mettl15* + METTL15' and 'Δ*Mettl15* + D169R METTL15' corresponds to the complementation of the *Mettl15* knockout cells by reintroduced intact or mutant *Mettl15* gene respectively. Mass of 1307 Da corresponds to fully methylated fragment, 1293 Da—fragment with one methyl group, 1279 Da—fragment without methyl groups. Peaks with masses of 1289 Da and 1275 Da corresponds to cyclophosphate forms of oligonucleotides with masses 1307 and 1293 Da respectively.

Similarity search (19) for the mammalian RsmH homologs resulted in identification of the single hit, methyltransferase METTL15 with e value $3{\cdot}10^{-62}$. METTL15 protein was previously identified as a component of mitochondria (20–22). It this work, we aimed to check whether murine METTL15 interacts with the mitochondrial 12S rRNA resulting in the formation of m^4C840 residue, determine the composition of the modification substrate and address the functional consequences of the lack of this modification. While we prepared the revision of this work, similar findings were reported by Minczuk (23) and Shi (24) groups.

MATERIALS AND METHODS

Cell culture

Mouse NS0 cells were cultured in RPMI 1640 medium (Gibco) supplemented with 10% FBS, GlutaMAX and

penicillin and streptomycin at 37°C, 5% CO_2. Large cell culture volumes were grown in Thomson Optimum Growth 1.6 l flasks in shaker-incubator at 110 rpm. NIH3T3, Hepa1-6 and Aml12 were cultured in DMEM/F12 medium (Gibco) supplemented with 10% FBS, GlutaMAX and penicillin and streptomycin at 37°C, 5% CO_2.

Mettl15 gene inactivation

Sequence of gRNA (5′-GCATACTGAATCTAAAGCT G-3′) for Cas9 targeting the first coding exon of *Mettl15* was generated using Benchling CRISPR guide RNA design tool (https://benchling.com).

Two complementary oligodeoxyribonucleotides containing the gRNA sequence and BbsI ligation adapters were annealed and ligated into BbsI-digested pX458 vector (25) (Addgene #48138). NS0 cells were transfected with the pX458 plasmid containing the gRNA sequence using Lipofectamine 3000 reagent (Thermo Scientific). Twenty four hours after transfection GFP-positive cells were sorted using BD FACS Aria III in 96-well plates containing 0.2 ml of RPMI medium per well. Individual clones were analysed by PCR amplification (primers 5′-GATTTCTTGACCTAC AAAATGCTTCG and 5′-TGTGGTGCCAAGCAATG AAC) of ∼250bp *Mettl15* fragment and sequencing of the amplicon. For off-target analysis we chose five off-targets with highest score according to the Benchling CRISPR guide RNA designing tool (https://benchling.com). Each off-target was analysed by PCR amplification of ∼250 bp region encompassing the area of partial complementarity to the gRNA. Sequences of possible off-targets and primers for PCR are presented in Supplementary Table S1.

Ectopic expression of *Mettl15* gene

Total RNA was isolated from NS0 cell line using PureLink RNA Mini Kit (Thermo Scientific). METTL15 cDNA was synthesized with reverse transcription by Maxima Reverse Transcriptase (Thermo Scientific) and specific primer (5′-GCCCCATACTTTACATTACATCCAG-3′) followed by PCR with Q5 High-Fidelity DNA Polymerase (NEB) using primers (5′-GGCCTCTGAGGCCATGCTTCGATAT CCATATTTTTACAGAAC and 5′-GGCCTGACAGG CCTCATAATTTGATGGCTGCTCTG). PCR product was ligated into SmaI-digested and dephosphorylated pUC19 vector. METTL15 ORF was then inserted into pSBtet-Neo (26) (Addgene #60509) by restriction free cloning using the following primers for the first PCR: forward 5′-TCGAAAGGCCTCTGAGGCCATG, reverse 5′-GCTTGGCCTGACAGGCCTC.

HRV 3C protease cleavage site and 3xFLAG tag were synthesized as primers (forward (METTL15) 5′-G CCAAGCTCAGAGCAGCCATCAAATTAGGCG GCAGCCTGGAGGTGCTGTTCCAGGGCCCTG ACTACAAAGACCATGACGGTGATTA-3′; forward (Luciferase) 5′-GCGGCAAGATCGCCGTGGG CGGCAGCCTGGAGGTGCTGTTCCAGGGCCC TGACTACAAAGACCATGACGGTGATTA-3′; reverse 5′-GAAGCTTGGCCTGACAGGCCTTACTTG TCATCGTCATCCTTGTAGTCGATGTCATGATC TTTATAATCACCGTCATGGTCTTTGTA-3′), which were hybridized and extended by Q5 High-Fidelity DNA Polymerase (NEB). Then they were used as megaprimers and inserted to the C-terminus of METTL15 or Luciferase by restriction free cloning (27). Obtained plasmid was used as template to create D169R mutation in *Mettl15* gene by PCR (forward 5′-AGGCTGGGGTGTTCTTCCATG-3′; reverse 5′-GCCCCATACTTTACATTACATCCAG-3′). PCR product then was circularised by T4 DNA ligase. To avoid possible mutations in the backbone of the plasmid *D169R-Mettl15* gene was inserted into pSBtet-Neo using SfiI restriction sites.

Mettl15 KO cell line and NS0 WT cell line were co-electroporated with plasmids coding for the FLAG-tagged METTL15, FLAG-tagged D169R METTL15 or FLAG-tagged Luciferase respectively and SB100x transposase (28) (pCMV(CAT)T7-SB100, Addgene #34879) in mass ratio 19:1 using Neon Transfection System (Thermo Scientific) according to manufacturer's instruction. Twenty four hours after electroporation cells were subjected to G418 (1 mg/ml, Thermo Scientific). Selection was carried out for 2 weeks and then cells were seeded to 96-well plates at an approximate density of 0.5 cell per well and cultivated in the medium without G418. For overexpression of FLAG-tagged METTL15 and D169R METTL15 we chose monoclonal cell lines with highest level of expression checked by western blotting with anti-FLAG antibodies.

12S rRNA isolation and MALDI MS

Total RNA was isolated using ExtractRNA reagent (Evrogen). 12S rRNA fragment was isolated using 5′-biotinylated oligodeoxyribonucleotide (5′-[biotin]- TGTTAAGTTT AATTTAATTTGAGGAGGGTGACGGGCGGTG) complementary to the region containing C840 of the 12S rRNA. Total RNA (2 mg/mL, 6 mg) and the oligonucleotide (200 pmol/ml) were heated in 6× SSC buffer for 5 min at 95°C and left in thermostat to anneal. After cooling to ∼37°C, RNase T1 (Thermo Scientific) was added to the mixture to the final concentration of 1 unit/ul and incubated for 1 h at 37°C. Then the solution was mixed with Streptavidin Sepharose High performance (GE Healthcare) and incubated 20 min at room temperature with rotation. The resin was washed three times with 3× SSC, 4 times with 1× SSC and 4 times with 0.1× SSC. 12S rRNA fragment was eluted from the resin by adding elution buffer (0.1× SSC, 6 M urea) and incubation for 5 min at 75°C. RNA from the eluate was precipitated with isopropanol overnight at –20°C. Precipitate was dissolved in 1× RNA Loading Dye (Thermo Scientific) and loaded on to 12% denaturing polyacrylamide gel. The gel was stained by ethidium bromide and the desired band was excised. The RNA band was fragmented and washed twice with the washing buffer (25 mM ammonium citrate, 50% acetonitrile) at room temperature for 10 min and dried with 100% acetonitrile.

For MALDI MS fragmented gel band was dried from acetonitrile in air at room temperature and RNA was digested with 1 unit/ul RNase T1 in 50 mM ammonium citrate for 3 h at 37°C. Digestion mixture (0.5 ul) was mixed with 50 mg/ml 2,5-dihydroxybenzoic acid in 0.5% trifluoroacetic acid and 30% acetonitrile (1.5 ul) and was left to

air dry at room temperature. MALDI mass spectrometry was performed in a reflector mode on an Ultraflextreame BRUKER equipped with a UV laser (Nd, 335 nm) detecting positive ions.

qPCR

For quantitation of different RNAs in WT and KO cell lines total RNA was isolated using PureLink RNA Mini Kit (Thermo Scientific). Total RNA was treated with DNase I (Thermo Scientific) followed by reverse transcription using Maxima First Strand cDNA Synthesis Kit (Thermo Scientific). SYBR Green PCR Master Mix (Thermo Scientific) was used to carry out real-time PCR reactions using Bio-rad CFX96 Touch Real-Time PCR Detection System. Each sample was run in triplicate and samples from four different experiments analysed in parallel. Primers sequences for analysis are the following:

12S rRNA – 5′-CTCAAAGGACTTGGCGGTAC, 5′-GTTTGCTGAAGATGGCGGTA;
16S rRNA – 5′-TGAAATTTCGGTTGGGGTGA, 5′-TCCCTAGGGTAACTTGGTCC;
18S rRNA – 5′-GTAACCCGTTGAACCCCATT, 5′-GGCCTCACTAAACCATCCAAT;
Gapdh – 5′-GGTCCCAGCTTAGGTTCATCAG, 5′-GTCGTTGATGGCAACAATCTCCAC.

Relative changes in transcript levels were calculated using the ΔCt method. The mean expression level of *Gapdh* was used for normalization.

For comparison of mtDNA copy number total DNA was isolated by phenol–chloroform extraction method and precipitated by ethanol. qPCR reactions were performed as described before. Each sample was run in triplicate and samples from four different experiments analyzed in parallel. Primers for 12S rRNA and 16S rRNA were the same as for the analysis of rRNA amount. Relative changes in DNA levels were calculated using the ΔCt method. The concentration of a single copy locus of the nuclear DNA (primers – 5′-CTTCCTTCTCTTACCTGCACGCC, 5′-GGTTACCAATGTCAGCGACGAGG) was used for normalization.

Immunoprecipitation

Cells were cultured in six 15 cm plates to the concentration of ∼2 × 10^6 cells/ml and then were transferred to a 1.6 l Thomson Optimum Growth Flask, volume was adjusted to 1 l, doxycycline hyclate (Sigma) was added to concentration of 1 ug/ml and the flask was placed in the shaker-incubator (37°C, 5% CO_2, 110 rpm). In 2 days, the cells were harvested, washed twice with 15 ml of PBS and kept frozen at –80°C prior to the immunoprecipitation (IP) experiment.

Cells were resuspended in 3 volumes of Nonidet-P40 buffer (25 mM HEPES–KOH, pH 7.5, 50 mM KCl, 10 mM $Mg(OAc)_2$, 0.5% Nonidet-P40) with Complete EDTA-free protease inhibitor cocktail (Roche) and lysed on ice for 30 min. Lysates were centrifuged for 15 min at 13 000 g at 4°C. Protein extracts were incubated with rotation for 2 h at 4°C with Anti-Flag M2 Affinity Gel (Sigma) which was prewashed 3 times with Nonidet-P40 buffer. Following incubation, beads were washed with Nonidet-P40 buffer 4 times. Elution was performed by shaking the resin with 20 ug of HRV 3C protease in 100 ul of Nonidet-P40 buffer for 2 h at 4°C.

Western blot analysis

For detection of the proteins the following antibodies were used: METTL15 antibody (PA5-65249, Invitrogen), C18orf22/RBFA antibody (ab224741, Abcam), RBFA antibody (PA5-59587, Invitrogen), MRPS34 antibody (PA5-59872, Invitrogen), MRPL13 antibody (PA5-51007, Invitrogen), MRPL48 antibody (ab194826, Abcam), CHCHD1 Polyclonal Antibody (MRPS37, PA5-90841, Invitrogen), anti-FLAG M2 antibody (F3165, Sigma), PTCD3 Polyclonal Antibody (MRPS39, PA5-59544, Invitrogen).

Mitochondrial protein synthesis

Mitochondrial protein biosynthesis was analyzed as described (29) with minor modifications. Briefly, ∼1 × 10^6 cells cultured at 37°C and in a 5% CO_2 atmosphere, in the appropriate medium, were harvested by centrifugation at 200g for 5 min, rinsed with 1 ml of PBS and resuspended in 1 ml of methionine-free medium supplemented with 200 ug/ml cycloheximide. After 5 minutes incubation at 37°C in a 5% CO_2, 5–10 uCi of EasyTag™ L-[^{35}S]-labeled methionine (Perkin Elmer) was added, and incubation continued for 45 min. The labeling was stopped by addition of cold methionine (final concentration 80 mM) and puromycin (final concentration 4 ug/ml). Cells were harvested, washed with PBS twice, resuspended in 100–150 ul of PBS and lysed with ultrasound. Protein concentrations were measured by a method of Bradford, equal amounts of total protein from different samples (30–50 ug) were applied to 15–20% gradient denaturing polyacrilamide gel. After electrophoresis at 25 mA for 5–6 h, gels were stained with Coomassie G-250, dried and analyzed by autoradiography with Storm 865 scanner (GE Healthcare). Gels images were analyzed using ImageJ software (NCBI).

Activity of respiratory complexes

NS0 cells were harvested at ∼10^6 cells/ml, 10^7 cells were washed with PBS, resuspended in respiration medium (0.137 M NaCl, 5 mM KCl, 0.7 mM NaH_2PO_4, 25 mM Tris–HCl solution with pH 7.4), incubated with 20 μg/ml digitonin 5 min at 37°C and were placed in Oxytherm (Hansatech, UK) chamber heated to 37°C. Stepwise control of the ETC-CI linked respiration was assessed using the protocol described in (30). Briefly, substrates or their precursors and then inhibitors of ETC complexes I (glutamate, malate – rotenone), II (succinate – malonate), III (glycerol-3-phosphate – antimycin A) and IV (TMPD, ascorbate – KCN) were added to the chamber consequentially. The next substance was added to the chamber when oxygen consumption rate was stable for 2 min. Activity of ETC complexes were calculated as difference in oxygen consumption rates after addition of substrate and inhibitor.

Sucrose gradient profiling of mitochondrial ribosomes

Mitochondrial ribosomes were isolated as described (31) with minor modifications. NS0 cells were grown to the concentration 1–2 × 10^6 cells/ml, washed with PBS and resuspended in MIB buffer (50 mM HEPES–KOH, pH 7.5, 10 mM KCl, 1.5 mM $MgCl_2$, 1 mM EDTA, 1 mM EGTA, 1mM DTT, protease inhibitors) and allowed to swell by stirring on ice. SM4 buffer (280 mM sucrose, 840 mM mannitol, 50 mM HEPES–KOH, pH 7.5, 10 mM KCl, 1.5 mM $MgCl_2$, 1 mM EDTA, 1 mM EGTA, 1 mM DTT, protease inhibitors) was added to adjust the final concentrations of sucrose and mannitol to 70 and 210 mM respectively. Lysis of cells in MIBSM buffer was done with Teflon Dounce homogenizer. Lysates were centrifuged at 800 × g 15 min at +4°C and supernatant was collected in new tube. The pellet after centrifugation was resuspending in half of the volume of MIBSM (3/4 of MIB and 1/4 of SM4) used in previous step and homogenization was repeated in such a way up to 4 times. All supernatants were combined. Mitochondria were pelleted from cell lysates by centrifugation at 10 000 × g for 15 min at +4°C, resuspended in SEM buffer (250 mM sucrose, 20 mM HEPES–KOH, pH 7.5, 1 mM EDTA) and loaded on top of the step sucrose gradient (2 ml 60%, 4 ml 32%, 2 ml 23% and 2 ml 15% sucrose in 20 mM HEPES–KOH, pH 7.5, 1 mM EDTA) in SW41Ti tubes (Beckman) and centrifuged in SW41Ti rotor at 27 000 rpm for 1 h at +4°C. Mitochondria (brown band migrating between 60% and 32% sucrose) were collected from tubes, resuspended in equal volume of gradient buffer without sucrose (20 mM HEPES–KOH, pH 7.5, 1 mM EDTA) and centrifuged at 10 000 × g 10 min at +4°C. Pellets of mitochondria were snap-freezed in liquid nitrogen and stored at –80°C.

For mitoribosome isolation ∼500 mg of mitochondria were used for each gradient. Mitochondria were defrosted in ice and lysed in two volumes of lysis buffer (25 mM HEPES–KOH, pH 7.5, 100 mM KCl, 20 mM $Mg(OAc)_2$, 2% Triton X-100, 2 mM DTT, protease inhibitors) for 10 min on ice. Lysates were cleared by centrifugation at 16 000 × g for 30 min at +4°C, then each 0.8 ml was loaded on top of 0.4 ml sucrose cushion (20% sucrose, 25 mM HEPES–KOH, pH 7.5, 50 mM KCl, 10 mM $Mg(OAc)_2$, 0.5% Triton X-100, 2 mM DTT) and centrifuged in MLA-130 rotor at 75 000 rpm for 2 h at +4°C. Pellet was resuspended in resuspension buffer (25 mM HEPES–KOH, pH 7.5, 50 mM KCl, 20 mM $Mg(OAc)_2$, 0.05% n-Dodecyl β-D-maltoside, 2 mM DTT), loaded on top of 10 ml of 10–30% sucrose gradient (25 mM HEPES–KOH, pH 7.5, 50 mM KCl, 10 mM $Mg(OAc)_2$, 2 mM DTT) and centrifuged in SW41Ti rotor at 24 000 rpm for 16 h.

Mitoribosome gradients were fractionated into 0.5 ml fractions using ACTA purifier (GE Healthcare) with monitoring absorbance at 260 nm. Proteins from 14 fractions of each gradient were isolated by TCA/deoxycholate precipitation as described in (32). Pellets were dissolved in equal volume of 1× Laemmli buffer and equal volume of each fraction was loaded on SDS page for western blot analysis. If several fractions were attributed to the single peak of either ribosomes, or the large or the small ribosomal subunits, they were combined and analyzed by mass spectrometry.

Proteome analysis

Eluates from the IP or fractions of gradients were loaded on to the 10% denaturing PAAG and when the proteins ran into the stacking gel current was stopped and the band containing total concentrated proteins was excised from the gel. Excised samples were washed twice with 10% acetic acid and 20% ethanol for 10 min, five times with HPLC grade water for 2 min and two times with 40% acetonitrile and 50 mM NH_4HCO_3. Then the pieces of gels were dried in acetonitrile. After gel drying on air they were trypsinized with Trypsin Gold (Promega) in 100 mM NH_4HCO_3 at 37°C for 4 h. Peptides were desalted using Pierce C8 Tips, 100 ul according to manufacturer's instructions. Peptides eluted from the tips were dried under vacuum and solubilized in 0.1% formic acid.

One microgram of peptides in a volume of 1–4 ul was loaded onto the Acclaim μ-Precolumn (0.5 mm × 3 mm, 5 μm particle size, Thermo Scientific) at a flow rate of 10 ul/min for 4 min in an isocratic mode of Mobile Phase C (2% acetonitrile, 0.1% formic acid). Then the peptides were separated with high-performance liquid chromatography (HPLC, Ultimate 3000 Nano LC System, Thermo Scientific, Rockwell, IL, USA) in a 15-cm long C18 column (Acclaim® PepMap™ RSLC inner diameter of 75 μm, Thermo Fisher Scientific, Rockwell, IL, USA). The peptides were eluted with a gradient of buffer B (80% acetonitrile, 0.1% formic acid) at a flow rate of 0.3 ul/min. Total run time was 90 min, which included initial 4 min of column equilibration to buffer A (0.1% formic acid), then gradient from 5 to 35% of buffer B over 65 min, then 6 min to reach 99% of buffer B, flushing 10 min with 99% of buffer B and 5 min re-equilibration to buffer A.

MS analysis was performed at least in triplicate with a Q Exactive HF-X mass spectrometer (Q Exactive HF-X Hybrid Quadrupole-Orbitrap™ Mass spectrometer, Thermo Fisher Scientific, Rockwell, IL, USA). The temperature of capillary was 240°C and the voltage at the emitter was 2.1 kV. Mass spectra were acquired at a resolution of 120 000 (MS) in a range of 300−1500 m/z. Tandem mass spectra of fragments were acquired at a resolution of 15 000 (MS/MS) in the range from 100 m/z to m/z value determined by a charge state of the precursor, but no >2000 m/z. The maximum integration time was 50 and 110 ms for precursor and fragment ions, correspondently. AGC target for precursor and fragment ions were set to 1 × 10^6 and 2 × 10^5, correspondently. An isolation intensity threshold of 50 000 counts was determined for precursor's selection and up to top 20 precursors were chosen for fragmentation with high-energy collisional dissociation (HCD) at 29 NCE. Precursors with a charge state of +1 and more than +5 were rejected and all measured precursors were dynamically excluded from triggering of a subsequent MS/MS for 20 s.

The obtained raw data were processed using the MaxQuant software (33) (version 1.6.10.43) with the built-in search engine Andromeda (34). In one run, all samples one biological replicate (for immunoprecipitation) or all samples of one cell line (gradient profiles) were analysed. Protein sequences of the complete mouse proteome provided by Uniprot (August 2019) was used for protein identification with Andromeda. Carbamidomethylation of cys-

teines was set as fixed modification and protein N-terminal acetylation as well as oxidation of methionines was set as variable modification for the peptide search. A maximum mass deviation of 4.5 ppm was allowed for precursor's identification and 20 ppm were set as match tolerance for fragment identification (acquisition in Orbitrap). Up to two missed cleavages were allowed for trypsin digestion. The software option 'Match between runs' was enabled and features within a time window of 0.7 min were used to match between runs. The false discovery rates (FDR) for peptide and protein identifications were set to 1%. Unique and razor peptides were used for label-free quantification (LFQ).

RESULTS

METTL15 methylates 12S mitochondrial rRNA

Mettl15 gene is encoded on a mouse chromosome 2. We compared *Mettl15* gene expression in a number of mouse cell lines, such as NIH 3T3, NS0, Hepa1-6 and Aml12 using RT qPCR (Supplementary Figure S1) and decided to proceed with NS0 cell line for further experimental analysis as this line possesses the highest *Mettl15* gene expression and is easy to handle to produce large amounts of biomass.

For *Mettl15* gene inactivation we generated a derivative of pX458 plasmid (25) coding for the components of CRISPR/Cas9 system directed to cleave *Mettl15* at its 45th codon. NS0 cells were transfected by the plasmid and seeded to monoclones by a fluorescence activated cell sorter. We obtained two monoclones with mutations disrupting *Mettl15* reading frame in all allelic variants (Supplementary Figure S2). To rule out an unlikely possibility that further observed phenotype might be caused by off-target mutations we checked the sequence of the five genomic regions carrying the most likely predicted gRNA binding sites outside *Mettl15* gene (https://benchling.com) and found out that there were no differences between WT and *Mettl15* knockout cell lines outside *Mettl15* gene (Supplementary Figure S3).

To check if *Mettl15* gene inactivation affected the 12S rRNA m^4C840 methylation we applied a combination of two previously published approaches (35,36). Total RNA isolated from the parental NS0 cell line and two independent *Mettl15* knockout cell lines was hybridized with the 5′-biotinylated 40mer oligonucleotide complementary to the 12S rRNA region containing m^4C840 residue. Excess of unhybridized RNA was digested with RNase T1 to trim 12S rRNA to the short oligomer and to remove other RNA species. After RNase removal and elution of RNA, the obtained 12S rRNA fragment was separated by a denaturing polyacrylamide gel electrophoresis. For the analysis of obtained RNA fragment, we developed an in-gel RNA cleavage procedure by guanylate-specific RNase T1 followed by the analysis of m^4C840 modification by mass spectrometry (Figure 1B). Our results demonstrate that 12S rRNA from *Mettl15* knockout cell line lacks C840 methylation resulting in the 14 Da mass shift in the corresponding (1293 Da) peak as compared with the WT (1307 Da). Moreover, we noticed that upon inactivation of the *Mettl15* gene not only C840 nucleotide became completely unmethylated, but also the neighbouring m^5C842 appeared to be methylated substoichiometrically, which leads to the 28 Da mass shift of the RNA fragment (Figure 1B). NSUN4 methyltransferase is known to be responsible for the formation of the 12S rRNA residue m^5C842 (37). Our results evidence for the coordination in the action of NSUN4 and METTL15 in modification of the decoding center of the mitochondrial ribosomes. In line with this observation substoichiometric formation of methylated 12S rRNA nucleotide m^5C841 (human numbering) was observed upon *METTL15* inactivation in a recent works of Minczuk (23) and Shi (24) groups.

To complement inactivation of the *Mettl15* gene in knockout cell lines we cloned *Mettl15* cDNA of the wild type NS0 cells to the pSBtet-Neo vector (26) capable of the random incorporation into the genome driven by a sleeping beauty transposase (28). As a negative control we created METTL15 catalytically inactive D169R mutant, likewise cloned into the same vector. After reintroduction of the *Mettl15* wild type or mutant genes into the population of knockout cells we repeated the analysis of the 12S rRNA modification and observed a partial restoration of m^4C840 modification in the case of the wild type, but not mutant *Mettl15* (Figure 1B).

Mettl15 interacts with an assembly intermediate of the 28S subunit of mitochondrial ribosome

Ribosomal RNA methyltransferases might interact with the ribosomal RNA at various stages of bacterial (38) and cytosolic (39) ribosome assembly starting from naked RNA and ending at the very late stages of assembly, in some cases even after subunit association into the ribosome (40). Some rRNA methyltransferases acting on bacterial (41–43) and cytosolic (44,45) ribosomes are functioning as assembly facilitating or quality control factors (3). Timing of the mitochondrial rRNA modifications is less clear. To get an idea on the particular mitochondrial 12S rRNA complex interacting with the METTL15 protein we supplemented NS0 cell lines with inactivated natural *Mettl15* gene by the gene coding for the FLAG-tagged METTL15 under doxycycline inducible promoter on a pSBtet-Neo vector (26) inserted into the genome by the sleeping beauty transposase (28). Copurification of the mitochondrial 12S rRNA, but not the mitochondrial 16S rRNA or cytosolic 18S rRNAs was detected by RT qPCR analysis (Figure 2A). Proteins copurified with METTL15 were analysed by mass spectrometry. LFQ intensities were used for quantification of proteins relative abundance (46). Identification of proteins coprecipitated with METTL15 (Supplementary Table S2, Figure 2B) revealed an almost complete set of the mitochondrial small ribosomal subunit proteins except for mS37, mS38 and mS39 (latter two were partially missed according to the mass spectrometry data). Lack of mS37 and mS39 in the assembly intermediate co-precipitated with METTL15 was confirmed by immunoblotting (Figure 2B). The proteins of the large mitochondrial ribosomal subunit were not found to be coprecipitated with METTL15. In addition, mitochondrial small ribosomal subunit assembly factor RBFA (47) and another mitochondrial rRNA methyltransferase, TFB1M (48), was found to be coprecipitated with METTL15, indicating that METTL15 target is most likely an assembly intermediate of the small subunit.

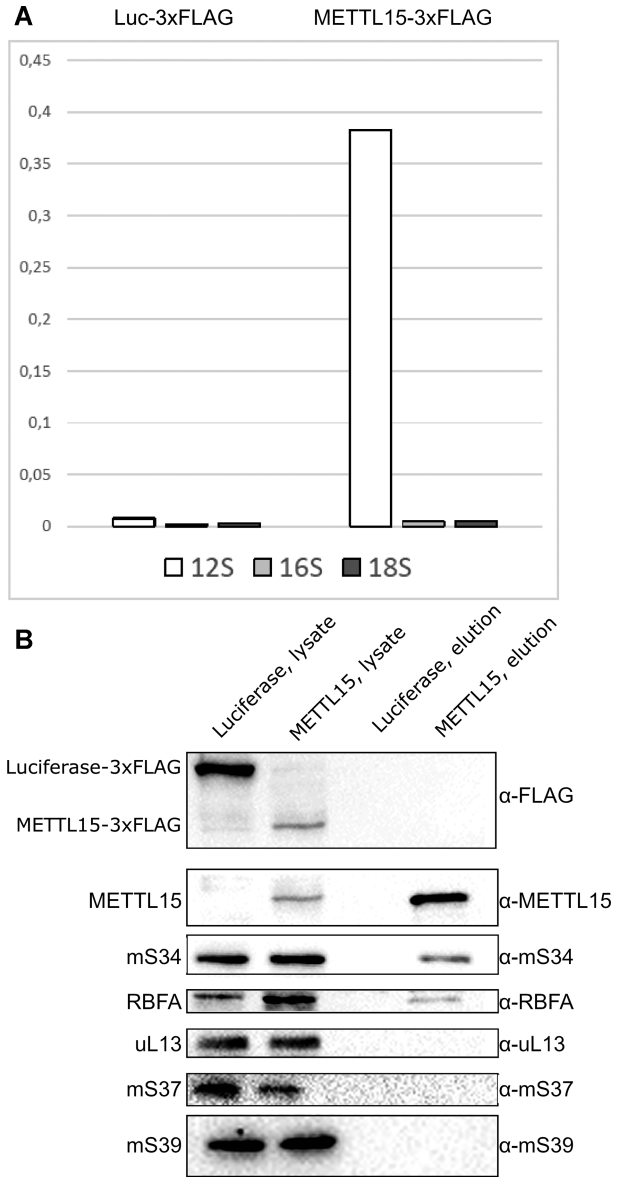

Figure 2. METTL15 interacts with the 12S rRNA, proteins and assembly factors of the mitochondrial small ribosomal subunit. (**A**) Amount of the 12S rRNA copurified with the FLAG-tagged METTL15 protein (right side) and FLAG-tagged luciferase as a control (left side). Mitochondrial large subunit 16S rRNA and cytosolic small subunit 18S rRNA were used for comparison. (**B**) Western blot analysis of METTL15 immunoprecipitation. The lanes are marked according to the FLAG-tagged protein (luciferase, METTL15) and the stage of purification (lysate, prior to purification; elution, sample co-purified with FLAG-tagged protein). The antibody used are listed on the right side of the panel, while identified protein bands are marked on the left side of the panel.

Lack of Mettl15 affects composition of the mitochondrial ribosomes

Bacterial rRNA methyltransferase genes have on average very moderate effect on the cell fitness (2,3) with the exception of antibiotic resistance methyltransferases (49,50) and methyltransferases reducing fitness cost of drug resistance (51). Inactivation of rRNA methyltransferases acting on the cytosolic (52) and mitochondrial (37,53) rRNA species might have deleterious effect. To compare the number of mitochondria in the wild type cells and cells with inactivated *Mettl15* gene we determined the amount of mitochondrial DNA (Figure 3A) and found it to be nearly the same. Lack of mitochondrial rRNA methyltransferase TFB1M results in a decrease of the 12S rRNA amount (53), likely due to its degradation. To check whether inactivation of the *Mettl15* gene would also result in the decrease in the 12S rRNA abundance we used RT qPCR (Figure 3B) and found no significant difference.

Role of the METTL15 methyltransferase in the efficiency of mitochondrial protein synthesis was assessed via [^{35}S]methionine incorporation into the proteins synthesized by the parental NS0 cells and *Mettl15* knockout cells while protein synthesis by the cytosolic ribosomes is inhibited by cycloheximide (Figure 3C, Supplementary Figure S4). No difference in the overall mitochondrial protein synthesis efficiency as well as in the proportions of the synthesized proteins encoded by the mitochondrial genome were revealed.

While the amount of mitochondrial proteins synthesized might be preserved, their functionality might be compromised e.g. with an increase in the frequency of translation mistakes. To evaluate the performance of the mitochondrial proteins synthesized by the ribosomes lacking the 12S rRNA m^{4}C840 residue modification we measured oxygen consumption rates of the permeabilized cells, sequentially supplied by the set of the substrates and inhibitors of the respiratory chain complexes I-IV (Figure 3D). No significant difference was found in the activity of respiratory chain complexes whose components were synthesized by the ribosomes lacking modification of C840.

While protein synthesis capacity of assembled mitochondrial ribosomes might be relatively tolerant to inactivation of the *Mettl15* gene, the efficiency of mitochondrial ribosome assembly might be affected. To this end we performed sucrose gradient centrifugations of the mitochondrial extracts from the parental NS0 cells, *Mettl15* knockout cell lines and knockout cells complemented by the intact and mutant *Mettl15* gene (Figure 4, Supplementary Figure S5). The amounts of free ribosomal subunits in the wild type and Δ*Mettl15* strains were barely distinguishable (Figure 4A, B). Ectopic expression of the wild type *Mettl15* gene resulted in higher proportion of the 55S ribosomes at the expense of free 39S and 28S subunits (Figure 4C). Increased ribosomal subunit association in this case is in a drastic contrast with the cells overexpressing the catalytically inactive D169R METTL15 mutant, where a substantial increase in the amount of free 39S and 28S subunits could be observed (Figure 4D).

To check whether protein content of the 39S and the 28S ribosomal subunits and the 55S ribosome is dependent on METTL15 methyltransferase activity we performed semi-quantitative proteome analysis of the sucrose gradient fractions to assess the presence of small subunit mitochondrial proteins (Supplementary Figure S6). RBFA assembly factor was observed mostly in the fraction of small ribosomal subunits of the wild type strain, but upon inactivation of the *Mettl15* gene was found in bigger amounts in the 55S ribosomal fraction (Supplementary Figure S6). This observation was confirmed by immunoblotting (Figure 4A, B,

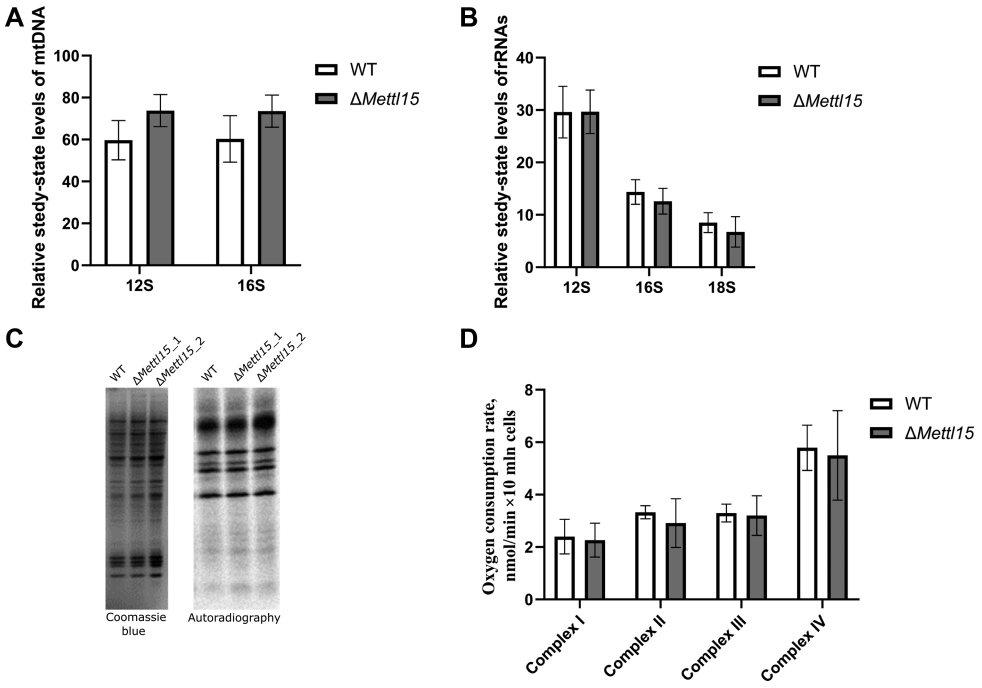

Figure 3. Inactivation of the *Mettl15* gene have very mild phenotype. (**A**) Comparison of mtDNA copy number in WT and KO cell lines determined by qPCR. A single copy nuclear DNA locus was used as a control ($n = 4$). (**B**) Comparison of the 12S rRNAs levels in WT and KO cell lines determined by qRT-PCR. Mitochondrial large subunit 16S rRNA and cytosolic small subunit 18S rRNA were used for comparison. Values were normalized to *Gapdh* mRNA ($n = 4$). (**C**) Mitochondrial protein synthesis in the WT and KO cell lines as revealed by [^{35}S]methionine inclusion (right panel) into proteins upon the cytosolic protein synthesis inhibition by cycloheximide. Coomassie staining (left panel) was shown as a loading control. (**D**) Comparison of the activity of respiratory chain complexes I–IV in the WT and KO cell lines ($n = 4$).

lower parts of panels). Even higher amounts of RBFA protein was found associated with the 55S ribosomes in the strain, expressing the D169R mutant form of METTL15 protein (Figure 4D, lower part of the panel). Additionally, we noticed an increase in the amount of 12S rRNA methyltransferase NSUN4 associated with the 55S ribosome, while the amount of NSUN4 associated with the 28S subunit decreased upon inactivation of METTL15 (Supplementary Figure S6).

DISCUSSION

METTL15 protein belongs to the conserved family of proteins (Supplementary Figure S7A) which are found in bacteria and majority of eukarya, but not archaea. As we demonstrated in this work and in consort with recent reports (23,24), eukaryal METTL15 protein is involved in the formation of m^{4}C840 residue of the 12S rRNA, a modification that is absent in the cytosolic ribosomes. Thus, taken into the consideration bacterial origin of mitochondria, it could be deduced that METTL15 and its bacterial homolog, RsmH, could recognize bacterial type of ribosomes, but not archaeal/eukaryal type. Lack of METTL15 homolog in yeast might likely reflect a loss of the gene in this lineage.

Structural analysis of the bacterial RsmH protein (54) revealed a Rossman fold methyltransferase core (Supplementary Figure S7A, structural elements marked green) with insertion of the substrate recognition domain (Supplementary Figure S7A, structural elements marked pink). Same architecture is conserved in the eukaryal METTL15 protein family variegated by a number of small size insertions in the loop regions of RsmH protein and appendage of the putative mitochondrial localization sequence at the N-terminus (Supplementary Figure S7A). Such a conservation makes it likely that RsmH/ METTL15 recognizes the same structural features of the small subunit conserved in both bacterial and mitochondrial ribosomes.

A possible explanation for the lack of m^{4}C1402/m^{4}C840 modification (Supplementary Figure S7B, left panel) outside bacteria/mitochondria might be the presence of m^{6}A1832 18S rRNA (human cytosolic ribosome numbering) modification in archaeal (55) and eukaryal cytosolic ribosomes (56) introduced by METTL5 (57). 18S rRNA nucleotide m^{6}A1832 forms a non-canonical base pair with Cm1703 (human cytosolic ribosome numbering) in a way that places the methyl group in the major groove of the RNA helix 44 (Supplementary Figure S7B, right panel) in direct contact with the phosphate group bridging nucleotides +2 and +3 of the P-site mRNA codon. The role of m^{4}C and m^{6}A at this site (Supplementary Figure S7B) might be similar, as was suggested for a number of other sites in the ribosome, where mutually exclusive modifications of the nucleotides neighbouring in 3D structure are observed in different evolutionary lineages (see (2) for a discussion). Alternatively, the role of these m^{4}C and m^{6}A might be different and specifically adapted to the mechanisms of translation initiation which are akin for bacterial and mitochondrial ribosomes (58) on one side vs. cytosolic and archaeal ribosomes (59) on the other. In line with

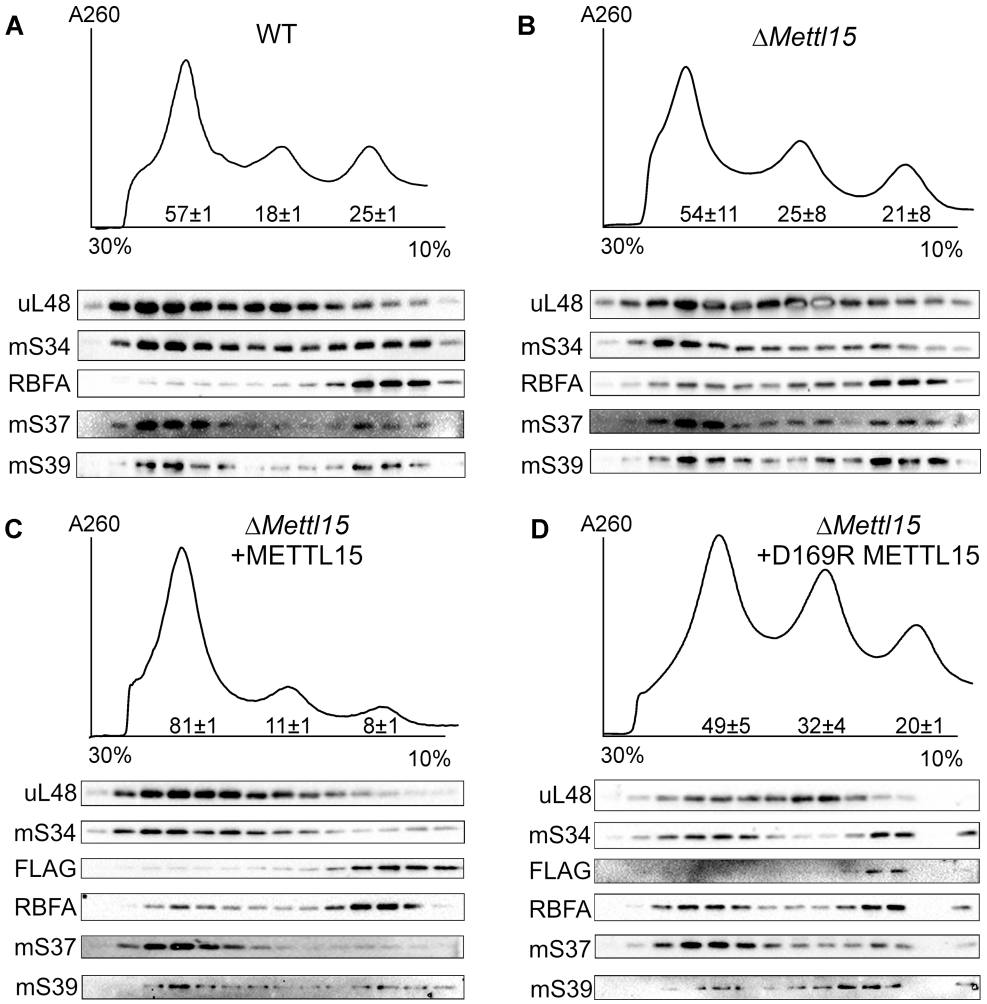

Figure 4. Influence of METTL15 methyltransferase on the mitochondrial ribosome assembly. (A–D) Shown are sucrose gradient profiles (upper panels) and immunoblotting of the individual gradient fractions (lower panels, proteins are indicated next to the gels) of the mitochondrial extract from the wild-type NS0 cells (**A**), Δ*Mettl15* cells (**B**) Δ*Mettl15* cells complemented with *Mettl15* gene (**C**) and Δ*Mettl15* cells complemented with mutant D169R *Mettl15* gene (**D**). Relative quantitation in percent based on 2–4 independent biological replicates are provided below the peaks.

this possibility is a decrease in initiation fidelity observed for *E. coli* lacking m^4C1402 modification (17). Whilst translation initiation fidelity assays for mitochondria remain undeveloped a role for the modification of m^4C840 of the 12S rRNA in initiation fidelity might be suggested as hypothetical. Moreover, it is hard to expect a significant phenotype due to hypothetical increase in misreading for the Δ*Mettl15* cells, since even for *bona fide* misreading mitochondrial ribosomes with a decrease in overall translation fidelity, there is no significant phenotype under cell culture conditions (60). While we have not observed a notable influence of the *Mettl15* gene knockout on the mitochondrial protein synthesis, it was described in recent publications (23,24). While an exact explanation for this discrepancy is unknown, it might be attributed to the species (mouse vs. human) or cell line (NS0 suspension diploid vs. HAP1 adherent haploid) specific difference.

The substrate for the METTL15 protein appeared to be an intermediate of the mitochondrial small subunit assembly, as revealed by copurification assay. This result fits well to the observation made for bacterial RsmH, which was shown to modify neither deproteinized 16S rRNA nor 70S ribosomes while showing suboptimal efficiency with completely assembled 30S subunit (17). In this work, we demonstrated that METTL15 interacts with the 12S rRNA in a complex with almost all small subunit proteins, but not the large subunit proteins. Lack of METTL15 interaction with the 55S mitoribosome is additionally supported by immunoblotting (Figure 4C, D) and mass-spectrometry (Supplementary Figure S6) of the sucrose gradient fractions. Thus, the substrate for the METTL15 is likely to be a late assembly intermediate of the 28S ribosomal subunit. TFB1M methyltransferase which is copurified with METTL15 is also known to act late in the process of assembly (53). The mS38 protein that was partially missed in the particle copurified with METTL15 is the closest protein to the site of modification, contacting the helix 44. This protein was reported (23) to be underrepresented in the small subunits of the human mitochondrial ribosomes from the line HAP1 with inactivated *METTL15* gene. This effect is not pronounced in NS0 murine cell line which we used, that perhaps might be attributed to the species or

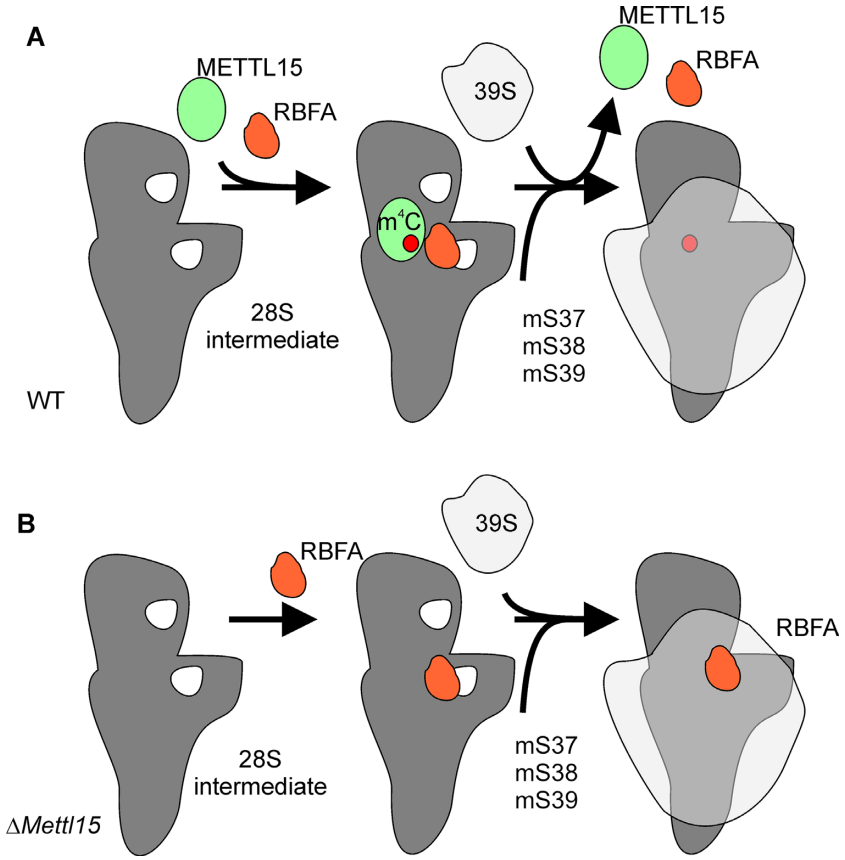

Figure 5. A scheme for METTL15 control over the late steps of mitochondrial small subunit assembly. Upper panel corresponds to the 28S subunit assembly in the wild type cells as suggested by the analysis of protein content of the METTL15 substrate complex, 28S and 55S gradient fractions of the WT cells. Relevant components, such as METTL15, r-proteins and RBFA are shown and labelled. Lower panel corresponds to the 28S subunit assembly in the *Mettl15* knockout cells as suggested by the analysis of protein content of the 28S and 55S gradient fractions of the Δ*Mettl15* cells.

cell line difference in the rate of mitochondrial ribosome biogenesis.

The mS37 protein which is completely missed in the complex with METTL15 is located on the back side of the small subunit connecting its head and the body (11) and might substitute bacterial 16S rRNA 3′-terminal region interacting with mRNA ribosome binding site (61). We found the RBFA protein, a homologue of bacterial ribosome assembly factor RbfA, as coprecipitated with the METTL15 methyltransferase, thus it is likely that the substrate for METTL15 methyltransferase is 28S assembly intermediate lacking mS37 and possessing smaller amounts of mS38 and mS39 while containing RBFA.

Apparently, METTL15 participate in the assembly of the small 28S mitochondrial ribosomal subunit. We detected only marginal increase in the amount of free ribosomal subunits in the Δ*Mettl15* cell line, in contrast to more pronounced effects observed by Minczuk (23) and Shi (24) groups. However, we observed an increase in ribosomal subunits amount in the cells with overexpression of the catalytically inactive D169R Mettl15 mutant. Expression of the catalytically inactive rRNA methyltransferases may lead to two types of consequences. For example, in the cases of Dim1 (45), WBSCR22 (62) and NEP1 (63), mutant rRNA methyltransferases might partially compensate for a deficiency of the corresponding natural gene. Exaggerated phenotype, caused by an expression of the catalytically dead methyltransferase, similar to the case of METTL15 observed here, was documented for bacterial KsgA methyltransferase (41). While in former cases the binding of methyltransferase might be hypothesized to fulfil the main assembly function, in the latter cases the dissociation of post-catalytic complex is presumably more important.

Of interest is a functional interaction of RBFA with METTL15. Bacterial RbfA was identified as high copy number suppressor of the cold sensitive mutation in the 16S rRNA (64). Inactivation of bacterial *rbfA* gene lead to a cold sensitive phenotype and accumulation of the 17S rRNA precursor (65). Bacterial RbfA binds 30S ribosomal subunit in the neck region with concomitant large, 25 Å relocation of the helix 45 and upper portion of the helix 44 (66). A functional interplay between the bacterial RbfA and 16S rRNA modification was previously demonstrated for the case of KsgA methyltransferase (67). Dislocation of the bacterial helix 44 region harbouring the RsmH modification site in a complex with RbfA might allow one to suggest a role for RbfA in creation a substrate for this rRNA methyltransferase.

While the process of mitochondrial small ribosomal subunit assembly is a way less studied than the assembly of its bacterial counterpart, the role of human RBFA in the pro-

Table 1. Enzymes responsible for the modification of the mammalian mitochondrial rRNA

12S rRNA	Enzyme/reference	Bacterial homolog
m^5U429	TRMT2B (68,69)	No
$m^4C839(m^4C840)$*	METTL15 (this study, (23,24))	RsmH (17)
m^5C841	NSUN4 (37)	RsmF** (70)
$m_2{}^6A936$, $m_2{}^6A937$	TFB1M (48)	KsgA (71)
16S rRNA		
m^1A947	TRMT61B (72)	No
Gm1145	MRM1 (73)	RlmB (74)
Um1369	MRM2 (73)	RlmE (42,43)
Gm1370	MRM3 (73)	No

*Human numbering, mouse numbering is provided in parenthesis.
***E. coli* RsmF modifies the nucleotide m^5C1407 of the 16S rRNA (70), which is proximal to C1404, equivalent to m^5C841.

cess of 28S subunit assembly is documented (47). Depletion of RBFA mRNA resulted in suboptimal dimethylation of the 12S rRNA residues A936 and A937 located in the helix 45 (47). On the basis of our results, we may hypothesize a similar cooperation of RBFA binding with the 12S rRNA m^4C formation. It is worth mentioning that in line with this idea, yeast lacking m^4C modification of mitochondrial rRNA also lacks a homologue of RbfA.

In the wild type cells, RBFA might be detected in the small subunit fraction, together with METTL15, while almost missing in the ribosome fraction. Inactivation of *Mettl15* gene result in the association of RBFA with the 55S ribosomes. It might be hypothesized (Figure 5), that completion of the 12S rRNA modification, following the late steps of the 28S subunit assembly, leads to displacement of both RBFA and METTL15 and engagement of newly made small subunits into translation. Without METTL15 this process is likely to be disordered so that subunit assembly intermediates containing RBFA might erroneously interact with the 39S subunits as evidenced from the analysis of the protein composition of sucrose gradient fractions. This conclusion is further supported by increased amounts of NSUN4 associated with the 55S ribosomes at the expense of its association with the 28S ribosomal subunit upon *Mettl15* gene inactivation. Decreased amount of NSUN4 associated with the 28S particles might explain suboptimal efficiency of the 12S rRNA m^5C formation by this enzyme in Δ*Mettl15* cell line.

As a summary of this work an updated table of enzymes responsible for the modification of mammalian mitochondrial ribosomes (Table 1) might be posted finalizing the entire list of proteins, aimed at modification of mitoribosomes.

SUPPLEMENTARY DATA

Supplementary Data are available at NAR Online.

FUNDING

Russian Science Foundation [19-14-00043 to P.S.]. Funding for open access charge: Skolkovo Institute for Science and Technology.
Conflict of interest statement. None declared.

REFERENCES

1. Boccaletto,P., Machnicka,M.A., Purta,E., Piatkowski,P., Baginski,B., Wirecki,T.K., de Crécy-Lagard,V., Ross,R., Limbach,P.A., Kotter,A. *et al.* (2018) MODOMICS: a database of RNA modification pathways. 2017 update. *Nucleic Acids Res.*, **46**, D303–D307.
2. Sergiev,P.V., Aleksashin,N.A., Chugunova,A.A., Polikanov,Y.S. and Dontsova,O.A. (2018) Structural and evolutionary insights into ribosomal RNA methylation. *Nat. Chem. Biol.*, **14**, 226–235.
3. Sergiev,P.V., Golovina,A.Y., Prokhorova,I.V., Sergeeva,O.V., Osterman,I.A., Nesterchuk,M.V., Burakovsky,D.E., Bogdanov,A.A. and Dontsova,O.A. (2011) Modifications of ribosomal RNA: From enzymes to function. In: Rodnina,M.V., Wintermeyer,W. and Green,R. (eds). *Ribosomes: Structure, Function, and Dynamics*. Springer Vienna, Vienna, pp. 97–110.
4. Brimacombe,R., Mitchell,P., Osswald,M., Stade,K. and Bochkariov,D. (1993) Clustering of modified nucleotides at the functional center of bacterial ribosomal RNA. *FASEB J. Off. Publ. Fed. Am. Soc. Exp. Biol.*, **7**, 161–167.
5. O'Brien,T.W. (2003) Properties of human mitochondrial ribosomes. *IUBMB Life*, **55**, 505–513.
6. Greber,B.J. and Ban,N. (2016) Structure and function of the mitochondrial ribosome. *Annu. Rev. Biochem.*, **85**, 103–132.
7. Boczonadi,V. and Horvath,R. (2014) Mitochondria: impaired mitochondrial translation in human disease. *Int. J. Biochem. Cell Biol.*, **48**, 77–84.
8. Singh,R., Sripada,L. and Singh,R. (2014) Side effects of antibiotics during bacterial infection: mitochondria, the main target in host cell. *Mitochondrion*, **16**, 50–54.
9. Böttger,E.C., Springer,B., Prammananan,T., Kidan,Y. and Sander,P. (2001) Structural basis for selectivity and toxicity of ribosomal antibiotics. *EMBO Rep.*, **2**, 318–323.
10. Greber,B.J., Bieri,P., Leibundgut,M., Leitner,A., Aebersold,R., Boehringer,D. and Ban,N. (2015) Ribosome. The complete structure of the 55S mammalian mitochondrial ribosome. *Science*, **348**, 303–308.
11. Amunts,A., Brown,A., Toots,J., Scheres,S.H.W. and Ramakrishnan,V. (2015) Ribosome. The structure of the human mitochondrial ribosome. *Science*, **348**, 95–98.
12. Agrawal,R.K. and Sharma,M.R. (2012) Structural aspects of mitochondrial translational apparatus. *Curr. Opin. Struct. Biol.*, **22**, 797–803.
13. Rorbach,J. and Minczuk,M. (2012) The post-transcriptional life of mammalian mitochondrial RNA. *Biochem. J.*, **444**, 357–373.
14. Bohnsack,M.T. and Sloan,K.E. (2018) The mitochondrial epitranscriptome: the roles of RNA modifications in mitochondrial translation and human disease. *Cell. Mol. Life Sci.*, **75**, 241–260.
15. Sirum-Connolly,K., Peltier,J.M., Crain,P.F., McCloskey,J.A. and Mason,T.L. (1995) Implications of a functional large ribosomal RNA with only three modified nucleotides. *Biochimie*, **77**, 30–39.
16. Baer,R. and Dubin,D.T. (1980) The 3′-terminal sequence of the small subunit ribosomal RNA from hamster mitochondria. *Nucleic Acids Res.*, **8**, 4927–4941.
17. Kimura,S. and Suzuki,T. (2010) Fine-tuning of the ribosomal decoding center by conserved methyl-modifications in the Escherichia coli 16S rRNA. *Nucleic Acids Res.*, **38**, 1341–1352.
18. Kiss-László,Z., Henry,Y., Bachellerie,J.P., Caizergues-Ferrer,M. and Kiss,T. (1996) Site-specific ribose methylation of preribosomal RNA: a novel function for small nucleolar RNAs. *Cell*, **85**, 1077–1088.
19. Altschul,S.F., Gish,W., Miller,W., Myers,E.W. and Lipman,D.J. (1990) Basic local alignment search tool. *J. Mol. Biol.*, **215**, 403–410.
20. Calvo,S.E., Clauser,K.R. and Mootha,V.K. (2016) MitoCarta2.0: an updated inventory of mammalian mitochondrial proteins. *Nucleic Acids Res.*, **44**, D1251–D1257.
21. Rhee,H.-W., Zou,P., Udeshi,N.D., Martell,J.D., Mootha,V.K., Carr,S.A. and Ting,A.Y. (2013) Proteomic mapping of mitochondria in living cells via spatially restricted enzymatic tagging. *Science*, **339**, 1328–1331.
22. Smith,A.C. and Robinson,A.J. (2016) MitoMiner v3.1, an update on the mitochondrial proteomics database. *Nucleic Acids Res.*, **44**, D1258–D1261.
23. Van Haute,L., Hendrick,A.G., D'Souza,A.R., Powell,C.A., Rebelo-Guiomar,P., Harbour,M.E., Ding,S., Fearnley,I.M., Andrews,B. and Minczuk,M. (2019) METTL15 introduces

N4-methylcytidine into human mitochondrial 12S rRNA and is required for mitoribosome biogenesis. *Nucleic Acids Res.*, **47**, 10267–10281.
24. Chen,H., Shi,Z., Guo,J., Chang,K., Chen,Q., Yao,C.-H., Haigis,M.C. and Shi,Y. (2020) The human mitochondrial 12S rRNA m^4C methyltransferase METTL15 is required for mitochondrial function. *J. Biol. Chem.*, doi:10.1074/jbc.RA119.012127.
25. Ran,F.A., Hsu,P.D., Wright,J., Agarwala,V., Scott,D.A. and Zhang,F. (2013) Genome engineering using the CRISPR-Cas9 system. *Nat. Protoc.*, **8**, 2281–2308.
26. Kowarz,E., Löscher,D. and Marschalek,R. (2015) Optimized sleeping beauty transposons rapidly generate stable transgenic cell lines. *Biotechnol. J.*, **10**, 647–653.
27. Bond,S.R. and Naus,C.C. (2012) RF-cloning.org: an online tool for the design of restriction-free cloning projects. *Nucleic Acids Res.*, **40**, W209–W213.
28. Mátés,L., Chuah,M.K.L., Belay,E., Jerchow,B., Manoj,N., Acosta-Sanchez,A., Grzela,D.P., Schmitt,A., Becker,K., Matrai,J. *et al.* (2009) Molecular evolution of a novel hyperactive Sleeping Beauty transposase enables robust stable gene transfer in vertebrates. *Nat. Genet.*, **41**, 753–761.
29. Fernández-Silva,P., Acín-Pérez,R., Fernández-Vizarra,E., Pérez-Martos,A. and Enriquez,J.A. (2007) In vivo and in organello analyses of mitochondrial translation. *Methods Cell Biol.*, **80**, 571–588.
30. Zhang,J., Nuebel,E., Wisidagama,D.R.R., Setoguchi,K., Hong,J.S., Van Horn,C.M., Imam,S.S., Vergnes,L., Malone,C.S., Koehler,C.M. *et al.* (2012) Measuring energy metabolism in cultured cells, including human pluripotent stem cells and differentiated cells. *Nat. Protoc.*, **7**, 1068–1085.
31. Aibara,S., Andréll,J., Singh,V. and Amunts,A. (2018) Rapid isolation of the mitoribosome from HEK cells. *J. Vis. Exp. JoVE*, **140**, 57877.
32. Reschke,M., Clohessy,J.G., Seitzer,N., Goldstein,D.P., Breitkopf,S.B., Schmolze,D.B., Ala,U., Asara,J.M., Beck,A.H. and Pandolfi,P.P. (2013) Characterization and analysis of the composition and dynamics of the mammalian riboproteome. *Cell Rep.*, **4**, 1276–1287.
33. Cox,J. and Mann,M. (2008) MaxQuant enables high peptide identification rates, individualized p.p.b.-range mass accuracies and proteome-wide protein quantification. *Nat. Biotechnol.*, **26**, 1367–1372.
34. Cox,J., Neuhauser,N., Michalski,A., Scheltema,R.A., Olsen,J.V. and Mann,M. (2011) Andromeda: a peptide search engine integrated into the MaxQuant environment. *J. Proteome Res.*, **10**, 1794–1805.
35. Golovina,A.Y., Dzama,M.M., Osterman,I.A., Sergiev,P.V., Serebryakova,M.V., Bogdanov,A.A. and Dontsova,O.A. (2012) The last rRNA methyltransferase of E. coli revealed: the yhiR gene encodes adenine-N6 methyltransferase specific for modification of A2030 of 23S ribosomal RNA. *RNA N. Y.*, **18**, 1725–1734.
36. Golovina,A.Y., Sergiev,P.V., Golovin,A.V., Serebryakova,M.V., Demina,I., Govorun,V.M. and Dontsova,O.A. (2009) The yfiC gene of E. coli encodes an adenine-N6 methyltransferase that specifically modifies A37 of tRNA1Val(cmo5UAC). *RNA N. Y.*, **15**, 1134–1141.
37. Metodiev,M.D., Spåhr,H., Loguercio Polosa,P., Meharg,C., Becker,C., Altmueller,J., Habermann,B., Larsson,N.-G. and Ruzzenente,B. (2014) NSUN4 is a dual function mitochondrial protein required for both methylation of 12S rRNA and coordination of mitoribosomal assembly. *PLoS Genet.*, **10**, e1004110.
38. Siibak,T. and Remme,J. (2010) Subribosomal particle analysis reveals the stages of bacterial ribosome assembly at which rRNA nucleotides are modified. *RNA N. Y.*, **16**, 2023–2032.
39. Sharma,S. and Lafontaine,D.L.J. (2015) 'View From A Bridge': a new perspective on Eukaryotic rRNA Base modification. *Trends Biochem. Sci.*, **40**, 560–575.
40. Ero,R., Peil,L., Liiv,A. and Remme,J. (2008) Identification of pseudouridine methyltransferase in Escherichia coli. *RNA*, **14**, 2223–2233.
41. Connolly,K., Rife,J.P. and Culver,G. (2008) Mechanistic insight into the ribosome biogenesis functions of the ancient protein KsgA. *Mol. Microbiol.*, **70**, 1062–1075.
42. Caldas,T., Binet,E., Bouloc,P. and Richarme,G. (2000) Translational defects of Escherichia coli mutants deficient in the Um2552 23S ribosomal RNA methyltransferase RrmJ/FTSJ. *Biochem. Biophys. Res. Commun.*, **271**, 714–718.
43. Bügl,H., Fauman,E.B., Staker,B.L., Zheng,F., Kushner,S.R., Saper,M.A., Bardwell,J.C. and Jakob,U. (2000) RNA methylation under heat shock control. *Mol. Cell*, **6**, 349–360.
44. Sloan,K.E., Warda,A.S., Sharma,S., Entian,K.-D., Lafontaine,D.L.J. and Bohnsack,M.T. (2017) Tuning the ribosome: the influence of rRNA modification on eukaryotic ribosome biogenesis and function. *RNA Biol.*, **14**, 1138–1152.
45. Lafontaine,D., Vandenhaute,J. and Tollervey,D. (1995) The 18S rRNA dimethylase Dim1p is required for pre-ribosomal RNA processing in yeast. *Genes Dev.*, **9**, 2470–2481.
46. Bantscheff,M., Schirle,M., Sweetman,G., Rick,J. and Kuster,B. (2007) Quantitative mass spectrometry in proteomics: a critical review. *Anal. Bioanal. Chem.*, **389**, 1017–1031.
47. Rozanska,A., Richter-Dennerlein,R., Rorbach,J., Gao,F., Lewis,R.J., Chrzanowska-Lightowlers,Z.M. and Lightowlers,R.N. (2017) The human RNA-binding protein RBFA promotes the maturation of the mitochondrial ribosome. *Biochem. J.*, **474**, 2145–2158.
48. Seidel-Rogol,B.L., McCulloch,V. and Shadel,G.S. (2003) Human mitochondrial transcription factor B1 methylates ribosomal RNA at a conserved stem-loop. *Nat. Genet.*, **33**, 23–24.
49. Cundliffe,E. (1978) Mechanism of resistance to thiostrepton in the producing-organism Streptomyces azureus. *Nature*, **272**, 792–795.
50. Lai,C.J. and Weisblum,B. (1971) Altered methylation of ribosomal RNA in an erythromycin-resistant strain of Staphylococcus aureus. *Proc. Natl. Acad. Sci. U.S.A.*, **68**, 856–860.
51. Freihofer,P., Akbergenov,R., Teo,Y., Juskeviciene,R., Andersson,D.I. and Böttger,E.C. (2016) Nonmutational compensation of the fitness cost of antibiotic resistance in mycobacteria by overexpression of tlyA rRNA methylase. *RNA N. Y.*, **22**, 1836–1843.
52. Lafontaine,D., Delcour,J., Glasser,A.L., Desgrès,J. and Vandenhaute,J. (1994) The DIM1 gene responsible for the conserved m6(2)Am6(2)A dimethylation in the 3′-terminal loop of 18 S rRNA is essential in yeast. *J. Mol. Biol.*, **241**, 492–497.
53. Metodiev,M.D., Lesko,N., Park,C.B., Cámara,Y., Shi,Y., Wibom,R., Hultenby,K., Gustafsson,C.M. and Larsson,N.-G. (2009) Methylation of 12S rRNA is necessary for in vivo stability of the small subunit of the mammalian mitochondrial ribosome. *Cell Metab.*, **9**, 386–397.
54. Wei,Y., Zhang,H., Gao,Z.-Q., Wang,W.-J., Shtykova,E.V., Xu,J.-H., Liu,Q.-S. and Dong,Y.-H. (2012) Crystal and solution structures of methyltransferase RsmH provide basis for methylation of C1402 in 16S rRNA. *J. Struct. Biol.*, **179**, 29–40.
55. Kowalak,J.A., Bruenger,E., Crain,P.F. and McCloskey,J.A. (2000) Identities and phylogenetic comparisons of posttranscriptional modifications in 16 S ribosomal RNA from *Haloferax volcanii*. *J. Biol. Chem.*, **275**, 24484–24489.
56. Piekna-Przybylska,D., Decatur,W.A. and Fournier,M.J. (2008) The 3D rRNA modification maps database: with interactive tools for ribosome analysis. *Nucleic Acids Res.*, **36**, D178–D183.
57. van Tran,N., Ernst,F.G.M., Hawley,B.R., Zorbas,C., Ulryck,N., Hackert,P., Bohnsack,K.E., Bohnsack,M.T., Jaffrey,S.R., Graille,M. *et al.* (2019) The human 18S rRNA m6A methyltransferase METTL5 is stabilized by TRMT112. *Nucleic Acids Res.*, **47**, 7719–7733.
58. Christian,B.E. and Spremulli,L.L. (2012) Mechanism of protein biosynthesis in mammalian mitochondria. *Biochim. Biophys. Acta BBA - Gene Regul. Mech.*, **1819**, 1035–1054.
59. Londei,P. (2005) Evolution of translational initiation: new insights from the archaea. *FEMS Microbiol. Rev.*, **29**, 185–200.
60. Akbergenov,R., Duscha,S., Fritz,A.-K., Juskeviciene,R., Oishi,N., Schmitt,K., Shcherbakov,D., Teo,Y., Boukari,H., Freihofer,P. *et al.* (2018) Mutant MRPS5 affects mitoribosomal accuracy and confers stress-related behavioral alterations. *EMBO Rep.*, **19**, e46193.
61. Mai,N., Chrzanowska-Lightowlers,Z.M.A. and Lightowlers,R.N. (2017) The process of mammalian mitochondrial protein synthesis. *Cell Tissue Res.*, **367**, 5–20.
62. Zorbas,C., Nicolas,E., Wacheul,L., Huvelle,E., Heurgué-Hamard,V. and Lafontaine,D.L.J. (2015) The human 18S rRNA base methyltransferases DIMT1L and WBSCR22-TRMT112 but not rRNA modification are required for ribosome biogenesis. *Mol. Biol. Cell*, **26**, 2080–2095.
63. Meyer,B., Wurm,J.P., Kötter,P., Leisegang,M.S., Schilling,V., Buchhaupt,M., Held,M., Bahr,U., Karas,M., Heckel,A. *et al.* (2011) The Bowen-Conradi syndrome protein Nep1 (Emg1) has a dual role in eukaryotic ribosome biogenesis, as an essential assembly factor and

in the methylation of Ψ1191 in yeast 18S rRNA. *Nucleic Acids Res.*, **39**, 1526–1537.
64. Dammel,C.S. and Noller,H.F. (1995) Suppression of a cold-sensitive mutation in 16S rRNA by overexpression of a novel ribosome-binding factor, RbfA. *Genes Dev.*, **9**, 626–637.
65. Xia,B., Ke,H., Shinde,U. and Inouye,M. (2003) The role of RbfA in 16S rRNA processing and cell growth at low temperature in Escherichia coli. *J. Mol. Biol.*, **332**, 575–584.
66. Datta,P.P., Wilson,D.N., Kawazoe,M., Swami,N.K., Kaminishi,T., Sharma,M.R., Booth,T.M., Takemoto,C., Fucini,P., Yokoyama,S. *et al.* (2007) Structural aspects of RbfA action during small ribosomal subunit assembly. *Mol. Cell*, **28**, 434–445.
67. Connolly,K. and Culver,G. (2013) Overexpression of RbfA in the absence of the KsgA checkpoint results in impaired translation initiation. *Mol. Microbiol.*, **87**, 968–981.
68. Laptev,I., Shvetsova,E., Levitskii,S., Serebryakova,M., Rubtsova,M., Bogdanov,A., Kamenski,P., Sergiev,P. and Dontsova,O. (2019) Mouse Trmt2B protein is a dual specific mitochondrial metyltransferase responsible for m5U formation in both tRNA and rRNA. *RNA Biol.*, **17**, 441–450.
69. Powell,C.A. and Minczuk,M. (2020) TRMT2B is responsible for both tRNA and rRNA m5U-methylation in human mitochondria. *RNA Biol.*, **17**, 451–462.
70. Andersen,N.M. and Douthwaite,S. (2006) YebU is a m5C methyltransferase specific for 16 S rRNA nucleotide 1407. *J. Mol. Biol.*, **359**, 777–786.
71. Poldermans,B., Roza,L. and Van Knippenberg,P.H. (1979) Studies on the function of two adjacent N6, N6-dimethyladenosines near the 3′ end of 16 S ribosomal RNA of Escherichia coli. III. Purification and properties of the methylating enzyme and methylase-30 S interactions. *J. Biol. Chem.*, **254**, 9094–9100.
72. Bar-Yaacov,D., Frumkin,I., Yashiro,Y., Chujo,T., Ishigami,Y., Chemla,Y., Blumberg,A., Schlesinger,O., Bieri,P., Greber,B. *et al.* (2016) Mitochondrial 16S rRNA Is Methylated by tRNA Methyltransferase TRMT61B in All Vertebrates. *PLoS Biol.*, **14**, e1002557.
73. Lee,K.-W. and Bogenhagen,D.F. (2014) Assignment of 2′-O-methyltransferases to modification sites on the mammalian mitochondrial large subunit 16 S ribosomal RNA (rRNA). *J. Biol. Chem.*, **289**, 24936–24942.
74. Lövgren,J.M. and Wikström,P.M. (2001) The rlmB gene is essential for formation of Gm2251 in 23S rRNA but not for ribosome maturation in Escherichia coli. *J. Bacteriol.*, **183**, 6957–6960.